GLINT

Gravitational-wave Laser INterferometry Triangle

TEAM RED : Shafa Aria, Rui Azevedo, Rick Burow, Fiachra Cahill, Lada Ducheckova, Alexa Holroyd, Victor Huarcaya, Emilia Järvelä, Martin Koßagk, Chris Mockel, Ana Rodriguez, Fabien Royer, Richard Sypniewski, Edoardo Vittori, Madeleine Yttergren
TUTOR : Martin Gehler

Abstract

The existence of supermassive black holes at the time when the Universe was only one billion years old is one of the mysteries of modern science. We do not understand the physical processes and evolution that took place in the early Universe and due to the limitations of receiving electromagnetic radiation from these regions we have not been able to study this interesting era. However, gravitational waves predicted by General Relativity provide us with the means to probe deeper into the history of the Universe. With GLINT we will be able to measure gravitational waves from the formation and evolution of the first black holes, with redshifts of $15 < z < 30$ *in the frequency range* $0.01 - 1\,\mathrm{Hz}$*. With a strain sensitivity of* $5 \times 10^{-24}\, 1/\sqrt{\mathrm{Hz}}$*, GLINT will also be sensitive to a host of other gravitational wave phenomena. The gravitational waves will be measured using laser interferometry to monitor the separation of test masses in free-fall. These test masses will be shielded from spurious forces in a constellation of three satellites in a geostationary orbit.*

1. Science with GLINT

Our current understanding of the Universe is based on the detection of electromagnetic radiation, which ranges from low-frequency radio waves, through the visible spectrum, to very high-energy gamma-rays. Electromagnetic radiation provides a useful but limited view into our Universe, since it interacts strongly with matter and it is susceptible to absorption and scattering. One of the most distant sources we have been able to observe are bright quasars which are believed to be powered by supermassive black holes (SMBH). So far over 40 quasars with redshift more than z=6 have been discovered (Wu et al. (2015) and references therein), each of them harbouring a black hole of several billion solar masses. The existence of supermassive black holes at that time, when the Universe was only one billion years old, is not easily explained with our current theories and is one of the most intriguing questions in science. Thus, evolution of the Universe during the first billion years is of high scientific interest.

Based on the theory of General Relativity, published by Albert Einstein in 1915, we know that there is another way to observe the Universe. General Relativity predicts that accelerating massive objects emit energy as gravitational waves. These propagate freely through the Universe at the speed of light and bring us information from the previously hidden era. With recent advances in technology this new window into the Universe is about to open : gravitational wave astrophysics will transform our understanding of the Universe.

With GLINT we will look at the formation and evolution of the first black holes during the billion years after the Big Bang. This mission will provide a better understanding of gravitational effects of massive objects.

Gravitational waves. When a massive object undergoes collapse it accelerates in space. If this collapse is asymmetric it creates ripples in spacetime, which propagate as waves. These waves are called gravitational waves and are characterized by the observer by their frequency, strain and polarization. Strain is the dimensionless fractional stretching and squeezing of spacetime as a gravitational wave passes.

gravitational waves are not absorbed by matter and so propagate throughout the Universe, and will therefore allow us to probe the Universe further than we can today using only electromagnetic radiation.

Indirect proof of the existence of gravitational waves comes from the observations of a binary pulsar PSR 1913+16, found in 1974 by Hulse & Taylor (1974). The orbital decay of the binary system due to the energy loss via gravitational wave emission is in excellent agreement with the predictions from General Relativity.

The first black holes. Black holes are formed when a massive star reaches the end of its life, and they have initial masses of low stellar-mass order. If the first black holes in the Universe were stellar-mass black holes they would have needed to constantly accrete at a maximum rate after their formation to become the supermassive black holes we observe at redshifts z>6. This scenario is highly improbable since different feedback mechanisms usually limit the black hole growth via accretion (e.g. Ricotti & Park (2012), however, see Madau et al. (2014)). Current theories predict that the formation of the first black holes might have been very different from what we see now in the local Universe.

Plausible scenarios for the early black hole formation are the collapse of supermassive stars (SMS), direct collapse black holes (DCBH) and the collapse of very massive objects (VMO).

Supermassive stars were some of the very first stars that were formed, called Population III stars. Due to environmental conditions in the early Universe they were able to reach masses of 260-800 $M_\odot$ and consisted solely of hydrogen. These massive stars were very short-lived and formed black holes with mass $M = 10^2 - 10^3\, M_\odot$ via core collapse (Fryer et al., 2002).

Direct collapse black holes are formed when a very massive gas cloud collapses directly into a black hole due to gravitational attraction. To form these black holes the gas must consist of atomic hydrogen. After the first direct collapse black holes formed they triggered further formation (Yue et al., 2014), resulting in a large amount of intermediate mass black holes (IMBH). These intermediate mass black holes are believed to either be embedded in galaxies or to have merged into supermassive black holes.

Very massive objects (Schneider et al., 2000) usually refer to either supermassive stars, which were already discussed, or clusters consisting of stars and gas. The clusters begin their collapse by merging a few stars and some gas, which leads to a runaway process where the mass continues to fall together, eventually resulting in a black hole of intermediate mass.

Evolution of black holes. When a black hole has been formed it will continue to grow through different processes : accretion, inspirals and mergers (Amaro-Seoane et al., 2012). Accreting black holes gather mass rather slowly and are limited by radiation pressure and feedback processes. Black holes can also grow through inspiraling of a stellar mass black hole, a neutron star or a white dwarf. The most efficient way to increase the mass is the coalescence of two black holes. The first black hole seeds experienced periodically intensive growth through these three processes, finally evolving to supermassive black holes.

Additional observable events. Besides the supermassive stars, the direct collapse black holes and very massive objects there are additional objects that GLINT can observe due to the frequency range that is studied. Amongst these are neutron star binaries and extreme mass inspiraling into a black hole. These objects are very important for testing General Relativity, and also to understand the specifics of how such systems behave.

Cosmology and theory of gravitation. One of the most important questions in cosmology in the present day is related to the composition of the Universe in terms of matter and dark energy densities. Using GLINT we can determine the direction and luminosity distance of long-lived sources (e.g. inspirals and binaries). If these gravitational wave sources emit radiation, like x-ray emission in inspirals or are located within host systems who also emit radiation, we can detect them with other electromagnetic wave observatories. Their redshift can be measured and by combining both measurements we can get a luminosity distance-redshift relationship, which in turn can provide constraints on the matter and dark energy densities.

Other on-going and planned observations (Planck, Euclid, LSST) that map the dark matter contents of the Universe may also assist this objective either directly or indirectly by providing corrections for the luminosity distance calculation.

Other missions

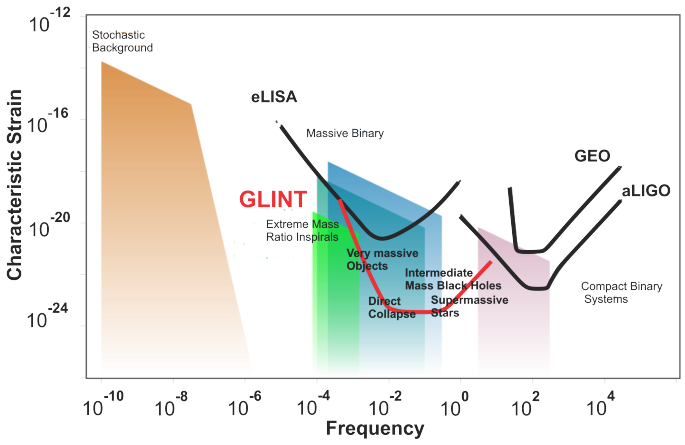

FIGURE 1: Illustration depicting the different sources. This is the gravitational wave spectrum with current and planned detector sensitivities superimposed.

There are other ways to study black holes, e.g. X-rays are emitted when matter falls into a black hole. But the redshifts studied here cannot be reached with that method nor any other, due to the limitations of electromagnetic radiation. Other gravitational wave antennas, such as LIGO, VIRGO and GEO600, are already in operation on Earth, but their sensitivity at low frequencies is limited by the arm lengths, seismic noise, and by interference from nearby moving masses.

At present there are two space-based missions planned for the near future : LISA (Laser Interferometer Space Antenna) and DECIGO (DECi-hertz Interferometer Gravitational wave Observatory). DECIGO is a proposed Japanese mission that will observe gravitational waves to study cosmology in a frequency range of $0.1 - 10Hz$ (Yagi, 2013), though it is still uncertain whether it will launch or not. The Laser Interferometer Space Antenna (LISA) is a ESA led project that will observe gravitational waves in a frequency range of $0.03\,\mathrm{mHz} - 0.1\,\mathrm{Hz}$. (Amaro-Seoane et al., 2012). The LISA mission's primary objective is to detect and measure gravitational waves produced by compact binary systems and mergers of supermassive black holes. In figure 1 the sensitivity and the frequency ranges for the different missions are illustrated, clearly indicating that GLINT will cover the gap in frequency range between existing and planned observatories with a significant strain sensitivity improvement.

1.1. Summary of GLINT Science

To provide a greater understanding of gravitational effects on massive objects, the GLINT mission will be addressing the following scientific questions about black holes :

- When the first black holes of several solar masses appeared,
- How they formed,
- What their properties were, and
- How they evolved (mergers, inspirals, accretion).

By analyzing the information obtained from answering these questions, we can find the rate at which black holes form. In addition to this, GLINT also has the ability to provide a greater understanding of massive binary systems

and to constrain cosmological models, and thus to answer these questions :

- How binary star systems of different masses behave,
- What pairs of objects (stars, black holes, etc) binary systems are made of.

Science with data from complementary experiments. With our instrumentation, we are also able to address the following :

- How the Universe evolved and what are dark matter and dark energy densities
- If the theory of General Relativity is the most applicable theory of gravitation

Using data obtained from other experiments (Athena, JWST), GLINT can corroborate and improve upon the current constraints for dark matter and dark energy densities taken from astronomical observations and more recently ESA's Planck mission (Planck Collaboration et al., 2014).

1.2. Scientific Objectives

To obtain the information needed to answer the above questions, we must measure :

- The direct collapse black holes in the range of 10^4-10^6 solar masses.
- The collapse of very massive objects in the range of 10^2-10^5 solar masses.
- The collapse of supermassive stars in the range of 260-800 solar masses.
- Two merging black holes in the range of 10^2-10^5 solar masses.
- Inspiraling of massive objects in the range of 100-10^3 solar masses.

2. Science Measurement and Instrumentation

To establish an extensive understanding of black hole formation and evolution we require comprehensive data from different black hole progenitor populations spanning redshifts : $z = 15 - 30$, as well as mergers of intermediate mass black holes and inspirals into black holes.
The theories and models predict the properties displayed in table 1.

Table 1: Wave detection parameters.

	SMS	VMO	DCBH
Required Sensitivity $(1/\sqrt{\text{Hz}})$	5×10^{-24}	10^{-23}	10^{-23}
Frequency (Hz)	0.4-1	0.01-0.2	0.01-0.1
Collapse duration (s)	5-60	10-100	10-100
Production rate/year	10^7	4000	10^4

To acquire the desired knowledge, GLINT must therefore measure the frequency and the strain of the gravitational wave, as well as the polarization of the wave. Without the polarization, we would be blind to a part of the wave. Besides providing the full amplitude of the wave the polarization also has information about the orbital frequency of binaries around their center of mass. Due to the short event duration and the potentially high event rate (see table 1), GLINT requires only one year of measurements to be able to collect enough data for meaningful analysis. Taking into account commissioning, safe modes and additional statistics for the science measurements, mission duration of 3 years has been designed.

The approximate positions of our target sources in a strain vs. frequency plot are shown in Figure 1.

2.1. Models of Formation and Evolution of Black Holes

To describe the gravitational wave emitted from the acceleration of a massive object a theoretical waveform can be constructed. These waveforms are distinct for each type of event. In figure 2 the waveform for the collapse of a $300\,M$ supermassive star is approximated, this is the lower mass range that GLINT will be able to detect. In figure 3 a theoretical model of the waveform of a direct collapse black hole is depicted and in figure 4 an illustration of the waveform of a massive object inspiraling and merging with a black hole is illustrated. The waveform of an inspiraling event is rather similar to the waveform of a merger, since both systems spiral before they merge, but the merger includes a ring down (a damping of the wave) after coalescence.

As the figures illustrate, the different events of black holes can be distinguished. There are extensive catalogues [1] with waveforms, e.g. (Saijo, 2011; Petrich et al., 1985) which can be used for analysing and describing the particular event depending on waveform observed.

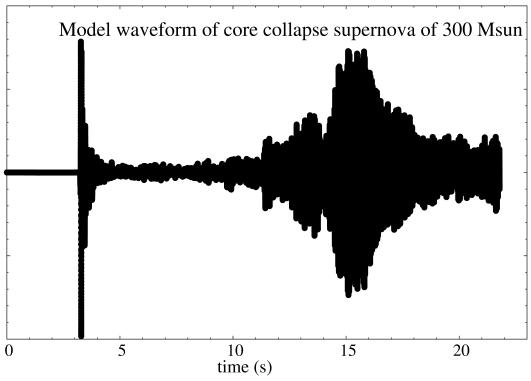

Figure 2: An estimated waveform for the gravitational wave emitted from a $300M$ super massive population III star, when collapsing into a black hole (Ott et al., 2006). The high amplitude emission at the first seconds is due to the bounce - the supernovae explosion. The y-axis is the strain which depends on mass, radius and red shift of the collapsing object. The x-axis depicts the timescale of the collapse in seconds.

2.2. How to Measure Gravitational Waves

Due to the nature of the gravitational waves a possible way to detect them is by measuring the distance changes between free floating bodies (see figure 5), i.e., only subjected to gravity. This has associated challenges : (i) achieve very low acceleration noise due to non-gravitational forces and (ii) measure the relative distance changes of the test masses very accurately. In GLINT this is done using laser heterodyne interferometry and is described in the following paragraphs.

The most currently popular technique for measuring gravitational waves is laser interferometry, which measures the change in distance between two objects caused by the

1. http://astrogravs.gsfc.nasa.gov/docSCatalog.html

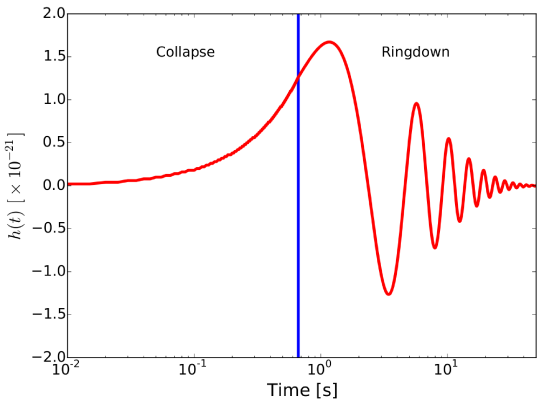

FIGURE 3: A theoretical model of the waveform of the gravitational wave emitted from a cloud of gas collapsing directly into a black hole (direct collapse black hole) (Pacucci et al., 2015).

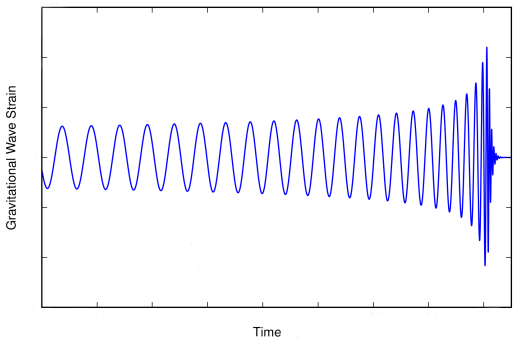

FIGURE 4: The gravitational wave from an object inspiraling into a black hole (Mohapatra et al., 2014) The increase in amplitude in the last part of the graph is due to the mergers approach.

passage of a gravitational wave. There are two main types : Michelson interferometry and Fabry-Perot interferometry.

Besides these there are other of proposed ideas e.g. atomic clocks (Graham et al., 2013), which measures the gravitational wave as a change in time, and Bose-Einstein Condensates (Sabin et al., 2014) that measures the change in phonon excitation generated by gravitational waves passing through. However, these proposals are purely theoretical without an experimental proof yet realized. Resonant bar detectors also have the potential to detect gravitational waves.

2.3. Mission Profile

Heterodyne interferometry concept. GLINT will use heterodyne laser interferometry to measure change in distances. Heterodyne laser interferometry provides the means to measure the phase between laser beams separated by a frequency in the MHz range (or any other that can be measured electrically). The two beams with different frequencies interfere when combined using a photo detector. The signal from the photo detector is a sine wave at the frequency difference. The phase changes of the signal are measured with a phase meter and indicate the relative phase between the beams which is directly proportional to the changes in distance : $\delta\phi = \frac{2\pi}{\lambda}\delta x$. This provides for very sensitive measurements assisted by the short wavelength of the laser, in our case 532 nm. The heterodyne interferometry system in GLINT is widely used to perform distance measurements and it is also the preferred option for other proposed gravitational waves observatories such as LISA (Danzmann, 2011). The measurement is performed indirectly in the following stages.

The measurement between the free floating test masses is split into three parts : test mass to optical bench distance, optical bench to optical bench distance and optical bench to test mass distance. They are described belowed.

Test mass to optical bench. The distance between the test mass and the optical bench measurement concept is shown in figure 6. Laser light is split in two beams with two different frequencies f_1 and f_2 by an acousto-optic modulator (AOM) by few MHz. The beam with frequency f_1 is reflected from the test mass and sent to the measurement photo detector where it interferes with the beam of frequency f_2. This generates a heterodyne signal (beat note) with a frequency $f_1 - f_2$. A phasemeter is used to measure the phase changes of the signal which is proportional to the displacement of the test mass because the beam at frequency f_2 has a fixed optical path. Similarly we measure a reference signal that is used to suppress common noise sources.

Optical bench to optical bench. In SC1 a frequency stabilized laser (master) sends light (10 W) to the SC2 by means of a large telescope as seen on figure 7. On SC2 the incoming beam interferes with the local laser. This signal is used to offset phase lock the laser on board to f_2 (around 10 MHz). Now the locked laser on SC2 sends light back to SC1 with 10 W of power. The incoming beam from SC2 interferes with the laser at SC1 generating a beat note signal at f_2, which contains a phase delay due to a passing gravitational wave. The phase is measured by a phasemeter.

Three spacecraft configuration. In order to be able to detect gravitational waves at least two arms are needed to create a virtual Michelson interferometer (see figure 7). For this reason one needs to measure the distances between SC1 and SC2 and SC1 and SC3 (or any other combination) and subtract them. However since the arm lengths are not the same the laser frequency noise degrades the measurement. Thus the distance between the SC has to be known to within 1 cm. This allows us to perform Time Delay Interferometry (TDI), which is done in post-processing by a combination of time delayed linear combinations of the signals.

Similar to the measurement between SC1 and SC2 the phase changes are measured between the SC1 and SC3. Finally, Doppler shifts have to be taken into account. They appear because of the relative velocities between the SC, which in our case are of $\pm 1.5\,\mathrm{m/s}$. This results in Doppler shifts of $\pm 3\,\mathrm{MHz}$ which are not a problem since f_2 and f_3 are set to 10 MHz and 8 MHz, respectively. This ensures that the beat node is always within photodiodes and phasemeter bandwidth.

The GLINT 3 SC configuration allows to use three interferometers (SC1-SC2-SC3, SC2-SC1-SC3 and SC3-SC2-SC1) see figure 7, which allows the measurement of the gravitational waves the polarization.

2.3.1. Noise analysis

A laser interferometric gravitational wave observatory in space consists of a virtual Michelson interferometer that measures changes in the distance between gravitational reference points : freely floating test masses that form the

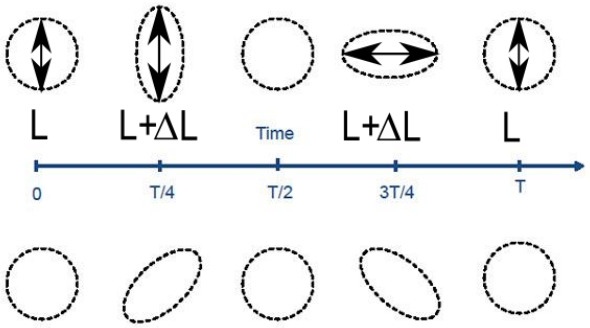

FIGURE 5: Change in distance between free floating bodies caused by a passing gravitational wave. Reference Neal (2015)

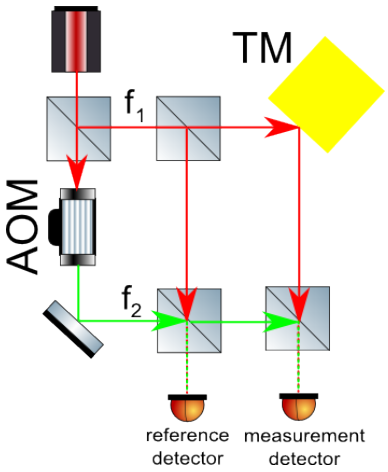

FIGURE 6: Measurement concept to determine the distance changes between test mass and optical bench. The "measurement detector" measures the phase changes caused by motion of the test mass while the reference detector is used as reference to minimize common noise.

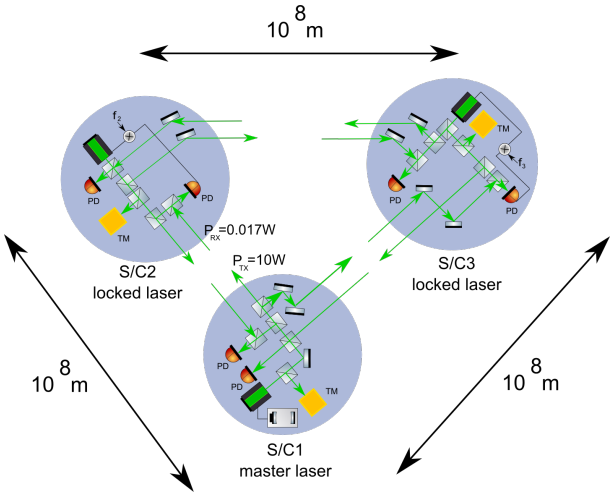

FIGURE 7: GLINT configuration and measurement concept to determine distance changes between the different SC.

end mirror of the interferometer arms in a Michelson-like configuration. The spacecraft follows a free floating mass by measuring the test mass position and actuating on the spacecraft position in a drag-free control. A free space laser link is established between the spacecraft.

As explained in section 1.2 a sensitivity of $\delta h = 5 \times 10^{-24} 1/\sqrt{\text{Hz}}$. For an armlength of 100 000 km this is equivalent to a displacement noise of $\delta x = 5 \times 10^{-16} \text{m}/\sqrt{\text{Hz}}$. Consequently, the noise levels of our measurement instrument must be below that.

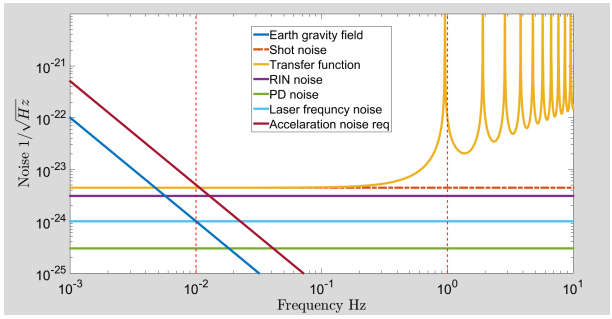

FIGURE 8: GLINT sensitivity curve including the most important sources of noise.

First we consider the performance of the interferometric measurement system. The transfer function describes how the gravitational waves couple to our instrument and it depends on the length of the arm length ($L_{\text{arm}} = 10^8$ m). There are multiple noise sources that are indistinguishable from an actual displacement due to a gravitational wave. The shot noise, which accounts for the fluctuations in the detected photon rate and the relative intensity noise, caused by fluctuations in the emitted laser power, deteriorates the interferometric measurement. To keep this error source below the threshold, a received power of 0.017 W is required. In order to accomplish that, 10 W of 532 nm laser light, with a RIN of 3×10^{-9} at MHz frequencies, is sent through the link and received by a 1.5 m diameter telescope.

The frequency noise of the lasers couples into phase fluctuations in the signal read-out. That is why one master laser is pre-stabilized by a reference cavity, to a level of $\delta\nu = 5\ \text{Hz}/\sqrt{\text{Hz}}$. All the others will be actively offset phase locked to the master laser. Further noise suppression will still be needed to achieve the required sensitivity. This is done with the already described time-delay interferometry (TDI), which requires an accuracy of 1 cm in the absolute positioning of the spacecraft. In addition, the optical bench requires a thermal stability of $\delta T = 0.1\,\mu\text{K}/\sqrt{Hz}$ in order to maintain the optical pathlength errors within the requirements. Finally, the noise levels of the phasemeter need to be $\delta\phi = 10^{-9}\ \text{rad}/\sqrt{\text{Hz}}$. Note that all the requirements only apply to the measurement band of the mission, from 0.01 - 1 Hz.(Barke, 2015)

The other key system of the mission is the quality of the free falling test masses. All residual forces acting on the test masses induce an acceleration noise that mimics the effect of a gravitational wave. The requirement for this noise source is $\delta a = 10^{-18}\,\text{m}/(\text{s}^2)\sqrt{\text{Hz}}$. Thermal radiation due to temperature differences, and radiation pressure exerted by the laser power sent to the mass are minimized to the requirement by using a test cubic mass of 7 kg and side 7 cm (Au-Pt alloy - density $2 \times 10^4\,\text{kg}/\text{m}^3$). The pressure in the mass assembly needs to be kept at $3 \cdot 10^{-7}$ Pa and a temperature of around 293 K within a thermal stability of $\delta T = 0.1\,\mu\text{K}/\sqrt{\text{Hz}}$. Magnetic forces need to be attenuated by a magnetic shielding so that the test mass, whose magnetic susceptibility and magnetic momentum are $\chi_{\text{mag}} = 10^{-7}$ and $m_r = 10^{-7}\,\text{A}/\text{m}^2$, respectively, is exposed to a maximal $\delta B = 0.07\,\text{nT}/\sqrt{\text{Hz}}$. Finally, the frequency band of the actuators (thrusters) needs to be shifted away to lower frequencies than the measurement band.

Figure 1 and 8 illustrates the influence of the mentioned

Table 2: Mass budget.

Subsystems	**Mass (kg)**
Thermal	26
Communications	17
Payload	627
Propulsion	193
Power	187
Bus	362
AOCS	47
Data handling	47
Total dry mass	1506
Propellant	75
TOTAL MASS	1581

noise errors in the sensitivity of the instrument. At high frequencies the sensitivity drops due to the transfer function of the interferometer. At intermediate frequencies the shot noise is the limiting error source. At low frequencies the acceleration noise limits the sensitivity.

2.4. Orbit

To detect gravitational waves from all directions with a frequency of $0.01 - 1$ Hz, a constellation of three satellites creating a triangle with an arm length of 100000 km is needed. All satellites will move in the same circular orbit with a semi major axis of 57 735 km but different true anomalies so they are shifted 120° from each other. This constellation is very stable, so the angle of 60° between the arms changes only about 0.04°. That means that the steering angle of the 1.5 m telescopes do not have to be changed. This would cause much distortion to the measurement process. Also the relative line-of-sight movement is less than 1.5 m/s. It is less than 10 m/s per year for orbit maintenance assumed. The orbit plane does not coincide with the ecliptic. So the interferometric measurement process is interrupted only 2 times a year for 14 days. This is in order to avoid the sun will shining within ±5° into the interferometer. In this phase the telescopes will be turned out of the sun. After the mission is finished there is no need for disposal because this orbit is 15.571 km behind the protected area of the GEO.

3. Spacecraft Design

3.1. Mass Budget

table 2 shows the mass budget calculated for each satellite, with a total mass of 1.581 kg including the propellant. A maturity margin has been included to account for the readiness of the technology. The payload is the largest contribution to the overall mass as this includes the telescope and the optical truss.

3.2. Power Budget

The primary power source is solar power, for which we use body mounted solar cells. There are every time effective 4,7 m^2 illuminated by sun. So 1582 W (BOL) will be generated for the subsystems and the batteries (32 kg). The solar cells used are 3G30C TJ solar cells from Azurspace with an efficiency of 30 %. The projected power consider also efficiency loss due to high temperature, micrometeoroids and

Table 3: Power budget.

Subsystems	**Power Consumption** (W)
Laser	300
Rest of system	50
Payload total	350
Propulsion	112
AOCS	50
Thermal control	350
Communications	20
Data handling	63
Platform total	665
Required power	965
System margin 20%	163
TOTAL POWER	1158

radiation. Several eclipse times occur twice a year. The duration of the longest eclipse lasts 70 minutes. To bypass it, there are eight VES16 Lithium Ion batteries from Saft in series to provide a 28 V bus voltage and 18+1 strings in parallel to provide 2432 Whr. This amount of energy maintains power losses during discharge and conversion and a depth of discharge of 70 % for more than 10000 cycles. The mode requiring the most power is the science mode with a total of 603 W, as this is when the lasers are in use and these have a large power consumption in order to meet the laser requirement. See table 3.

3.3. Structural Design

The structural design of GLINT spacecraft, shown in figure 9, is composed of three main parts : the structural frame and its plate, the payload section, and the walls and shielding. The lower part of the spacecraft (main structural frame) is used to endure the mechanical loads and the vibrating environment during the launch and the cruise. It is equipped with apogee thrusters and supports the components of the service module. Its design is inspired by the MSL Skycrane vehicle. The upper part of the spacecraft is occupied by a big torus directly mouted on the main plate of the lower frame (inspired by the Gaia spacecraft). It supports the mirrors, the optical bench and the test mass unit, and prevent the payload from being perturbed by the other units and bring stability. Four structural cylinders carry the walls and the top and stand the compression load induced by the weight of the two other spacecrafts fixed on it. The Attitude and Orbit Control System thrusters and star trackers are fixed on the walls. The adapter on the top forms the interface between the spacecraft during launch. The diameter of the spacecraft is 4.5 m and the height is 3 m.

3.4. Thermal Subsystem

The spacecraft is exposed to several heat sources : solar radiation, Earth reflection, infrared radiation from Earth and internally dissipated electrical energy. Thermal design is required to maintain the optimal temperature of the spacecraft. The temperature of the spacecraft is 25°C for the hot case. Because of the great thermal mass and a black Multi Layer Insulation (MLI) the average temperature is 22 °C during the maximum eclipse of 70 minutes. This

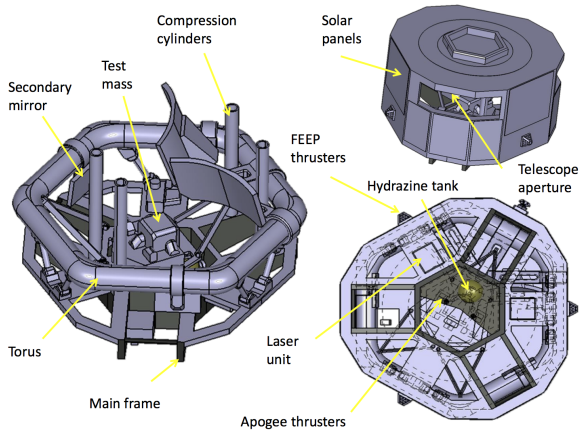

Figure 9: Structural Design

temperature can also be increased by heaters. To monitor the temperature, there are four 100 Ω thermistors and two thermocouples. The payload itself requires a thermal stability of 100 nK at a frequency of 10^{-2} Hz. While this may be a challenging requirement, temperature noise decreases rapidly with increasing frequency. Heaters, thermal isolation and structural materials with a small thermal expansion coefficient are used to maintain this. GLINT benefits from operating at a higher frequency so this requirement should be achievable.

3.5. Propulsion System

In the following subsections we will discuss the drag force and the spacecraft thrusters.

3.5.1. Drag Free Control

Gravitational wave detection requires the determination of extremely small strains, and high precision control, therefore, moving to space provides an opportunity to be free of fundamental low frequency limitations from gravity gradient effects on the Earth. However, a satellite's orbit is disturbed by residual air drag, radiation pressure, micrometeorite impacts, solar wind and other small forces that act on its surface. Using drag-free control will attenuate these non-gravitational forces to acceptable levels in order to provide a dynamically quiet platform for high-precision experiments (Funakki & Nakayama, 2011).

There are at least three potential ways to utilize a drag-free satellite for scientific purposes. The first is that the test mass is unsupported and protected from outside disturbances and therefore is in a particularly benign environment. Secondly, the path of the satellite is purely gravitational providing an improved measurement of the gravitational field. Thirdly, the thrusters produce forces equal and opposite to the disturbances and thus are a measure of these external disturbances with improved bandwidth and accuracy compared with measuring the effect on a satellite's orbit (DeBra, 1997).

3.5.2. Micropropulsion Thrusters

In order to provide a high-precision measurement in the spacecraft, it is required to have at least a thrust precision of 0.5 μN and a thrust noise of 0.1 $\mu\text{N}/\sqrt{\text{Hz}}$. Only a few thrusters are qualified in terms of thrust level, thrust precision, and thrust noise. The best candidate for this mission are the Field-emission electric propulsion (FEEP) thrusters.

Table 4: FEEP Characteristics

Thrust, range per unit	0.3-150 μN
Propellant	Ce, In
Thrust Accuracy	0.1 μN
Thrust Response	0.1 ms
Thrust Noise	$<0.1\,\mu\text{N}\sqrt{\text{Hz}}$
ISP	4000-8000 s
System Weight	>14 kg
Lifetime	>4000 h
Thrust Control	Accelerate Voltage

FEEP is an advanced electrostatic space propulsion concept, a form of ion thruster, that uses liquid metal (usually either cesium, indium or mercury) as a propellant. A FEEP device consists of an emitter and an accelerator electrode. A potential difference of the order of 10 kV is applied between the two, which generates a strong electric field at the tip of the metal surface. The interplay of electric force and surface tension generates surface instabilities, which give rise to Taylor cones on the liquid surface. At sufficiently high values of the applied field, ions are extracted from the cone tip by field evaporation or similar mechanisms, which then are accelerated to high velocities (typically 100 km/s or more) (Marcuccio & Genovese, 1998). Described specifications can be seen in the table 4.

3.6. Drag Free Attitude Control System (DFACS) and Attitude Control (AOCS)

During the science mode the spacecraft follows the movement of the test mass on its geodesic trajectory using its drag free attitude control system with the FEEP thrusters described in 3.5.2. Outside of science mode, the attitude of every spacecraft is measured by a three-headed star tracker. In case of safe mode, the attitude is detected by two sun sensors and an Inertial Measurement Unit (IMU). For attitude control the three stacks of FEEP thrusters are used. Every stack consists of four thrusters, providing torque-free and pure torque control.

3.7. Data Handling

The command and data handling subsystem, C&DH, performs two major functions. It receives, validates, decodes and distributes commands to other spacecraft systems and gathers, processes, and formats spacecraft housekeeping and mission data for down-link or use by an on-board computer. The communication link to the Earth allows data to be sent at a speed of around 2048 kbps for approximately 2 hours a day. A maximum data transfer of 1.8 GB per day is thus reasonable. Temporary storage of the data is needed as well as access to a flexible on-board computer. Each of the spacecraft data handling architecture is centered on the Thales Leonardo architecture with estimated power consumption of 33 W and a mass of 10.2 kg, including internal redundancy. The main tasks of the on-board computer are decoding of the telecommands from the ground and ensuring their execution, on-board housekeeping and scientific data telemetry formatting for transmission, overall data management, execution of the attitude and orbit control system software.

Internal Mass Memory of 32 GB end of life is for housekeeping and science data is already included in the CPU unit as the data amount which needs to be temporarily stored on the Mass Memory Unit (MMU) is small enough so that additional MMU is not required. There is also one Remote Terminal Unit (RTU) which is the interface between the main on-board computer and the payload and different subsystems platform units with power consumption 30 W and a mass of 10 kg. Instructions to subsystem units and telemetry back from them are passed through a 1553 bus. The payload, which generates larger volumes of data, has its own dedicated channel. The network communication between CPU and the RTU is done via Space Wire. The system is compatible with the radiation environment in GEO type orbits.

3.8. Telecommunication

The TT&C subsystem is dedicated to the retrieval of telecommands and the transmittance of telemetry. The telemetry data consists of the housekeeping data of the subsystem including information on voltages, currents, pressures, temperature, operational states, etc. The scientific data acquired by the payload of the spacecraft is down-linked to the ground stations. The data transmission/reception is performed by X band low-gain patch antenna, each of the three satellites will carry 3 patch antennas to cover all directions when orbiting around Earth. The antenna gain for down-link is 3 dB.

3.8.1. Data Rates and Down-link

The net effective continuous data rate for each instrument of the constellation is 57 kbps of which 15 kbps is housekeeping data and 42 kbps is science data. Transmitting shall be done by X band with frequency 8.45 GHz. The orbit specification with a maximum spacecraft to ground station distance of 57 274 km and communication schedule foresees on average 2 hours for each satellite of contact every 3rd day (with 17 hours per day download windows available) with a actual down-link rate of 2048 kbps, resulting in an average daily data volume of 1.8 GB from each satellite and a total daily data volume 5.5 GB. For the nominal observation time of three years the total data amount shall be of about 6 TB. No on-board reduction of the data will take place.

4. Ground Segment Infrastructure

4.1. Ground Segment

The ground segment provides capabilities for monitoring and controlling the spacecraft and payload during all phases of the mission, as well as for the reception, archiving and distribution of the data gathered by the payload instruments. The telemetry, tele-command and tracking operations are established with ESTRACK's 35 m ground stations at Malargüe (Deep Space Antenna DSA 3) which is part of the European Deep Space Network. The 35 m station provide the improved range, radio technology and data rates required by current and next-generation exploratory missions. Selected ground station is able to receive X-Band signals which shall be used for the GLINT mission. The Mission Operations Centre will be located at ESOC in Darmstadt, Germany. The Science Operations Centre supports the scientific mission planning and experiment command request preparation for consolidated onward submittal to the Missions Operations Centre. The SOC will process data and he ground segment of GLINT consists of a ground station, Mission Operations Centre and a Science Operations Centre. It provides capabilities for monitoring and controlling the spacecrbuild the data archive for the scientific community. The exisiting ESA/ESOC ground segment elements and facilities available through other space missions like Rosetta or Venus Express can be reused for the GLINT mission as well.

4.2. Post Processing

In order to satisfy the scientific goals of the mission we need a strain sensitivity level of $\lesssim 5 \cdot 10^{-24}\, 1/\sqrt{\mathrm{Hz}}$ by using laser interferometry. The fractional frequency stability of the pre-stabilised laser source is approximately assumed to be $10^{-14}\, 1/\sqrt{\mathrm{Hz}}$ requires further error correction to achieve the requirement. It must be taken into account that, due to relative movements between the spacecraft, the distance of the interferometer arm is expected to change approximately $\pm 0.03\%$ over one orbit. As consequence, the resulting unequal arm configuration of GLINT turns laser frequency into excess noise added to the measured phase, which could spoil the scientific performance of the mission. There are three approaches to reduce the noise to the required sensitivity : pre-stabilization, arm locking and time delay interferometry (TDI) (Livas et al., 2009). With TDI we can cancel laser frequency noise by combining the phase measurements made at different times. Synthesizing and equal-armlength interferometer that is insensible for frequency noise. Matched filtering can be used as a next step which can recognize signals of an expected form. An example how it can be done can be see in Bender (1998) The required timing of the measurement is set by the light travel times between the GLINT spacecraft and it has to be better than 33 ps, corresponding to 1 cm, to meet the laser frequency noise suppression requirement. For further information see Shaddock et al. (2008) and Armstrong et al. (2002).

5. Launch

The mass of each spacecraft is 1.581 kg. So it is possible to launch 3 satellites with one rocket, to save cost. A rocket like Ariane 5 Me or similar is therefore for recommended (Schilling, 2009). The long fairing of the Ariane 5 can cover all three satellites (Perez, 2011). The inclination of the target orbit of the 3 satellites is nearly arbitrary. So an inclination of 12° for a maximum lift of mass of the launcher is chosen. The upper stage of the launcher will release the satellites in 3 slightly different orbits and have to be capable for multiple ignitions for this purpose. GLINT 2 will be released in the target orbit with an eccentricity of 0 and a semi major axis of 57735 km. GLINT 1 and GLINT 3 have an eccentricity of 0.023 and 0.022 a semi major axis of 56444,8 km and 59011 km. So they can drift away from each other. After 15.6 respectively 16.5 days both satellites drift to a position 120° displaced from GLINT 2. According to calculations in Satellite Tool Kit (STK) form AGI an apogee burn of two 20 N thruster will achieve a delta-V of 30.21 m/s respectively 28.25 m/s to circulate the orbits of the both spacecraft. Now an orbit constellation of an equilateral triangle with an arm length of 100 000 km is

created .The propellant mass for each spacecraft will be about 75 kg of hydrazine. (Airbus, 2003)

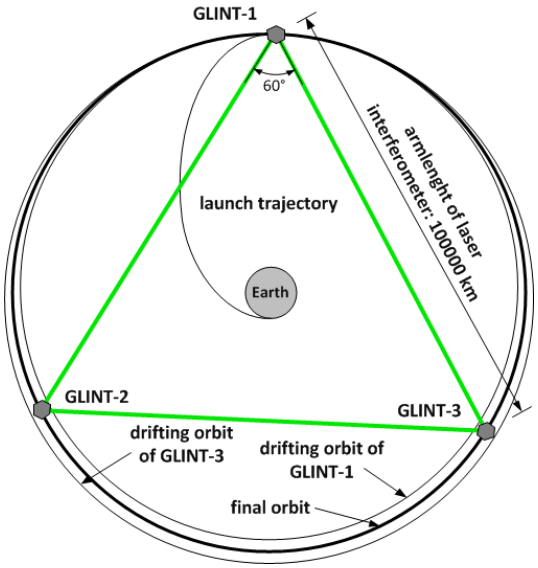

Figure 10: Orbit

6. Alternative Proposals

During early mission development a small team researched an alternative proposal, which proved to need too many immature technologies to be feasible. Still using laser interferometry and a triangular satellite constellation, the novelty is the use of Fabry-Perot type interferometer which has the major advantage of combining an enormous accuracy with short arm-lengths : 1000 km. A Fabry-Perot interferometer consists of two mirrors with which to bounce the laser beam back and forth, thus simulating a longer arm-length. The major complication with this setup in space consists in keeping the cavity between the two mirrors as constant as possible.

7. Development Costs

7.1. Risk

Technically, a large proportion of the risk to the mission lies in the requirement to perform interferometry at larger distances in space. During mission design we evaluated several scenarios that could represent possible risks for our mission. The most important ones are :

FEEP's malfunctions, which leads to loss accuracy during the measurements ; number of spacecraft's in orbit operation (three in total), mainly because the probability of an undesired event during the operational phase of the mission increases with the number of spacecraft ; problems in the test masses or lasers in the interferometry, losing accuracy in the measurement ; aberrations in the telescopes lens like Hubble telescope had in the 90's ; wrong orbital injection which leads to lose accuracy in the interferometry operation or lose one spacecraft in the worse case scenario.

7.2. Total Cost

GLINT is a large mission that will be launched with an Ariane 5 rocket from European Space Agency. The overall estimated budget is around 2100 M€ for a three year long mission. In table 5, there is an estimate of the costs. The lasers, telescopes and mirrors will be very expensive as they require high precision and sensitivity. The mission has three spacecraft thus driving the cost.

Table 5: Development costs.

	Millions of €
Optical Bench	200
Launch	150
Operations	120
ESA	80
20 % margin	350
Spacecraft	1200
TOTAL COST	2100

7.3. Descoping Options

If we have to descope because of budgetary constraints, we could eliminate one of the arms. Thanks to this we will economize by eliminating two telescopes which are one of the most expensive components of the mission. On the other hand, we would lose the polarization of the gravitational waves, which would significantly hamper the information on the sources that we can extract from the waveforms, and we would not have redundancy in case of loss of one of the arms for the other measurements. Other descoping options include reducing the size of the telescopes or making cuts in noise reducing components. It would still be possible to make some measurements on some of the primary objectives, but the number of observed event would drop drastically and we might not be able to complete some of our primary objectives.

8. Timeline and Verification Matrix

In comparison to other missions that are scheduled for future, our mission will require a higher sensitivity of an order of $10^{-24}\,1/\sqrt{\text{Hz}}$. The mission is thereby four orders of magnitude higher in sensitivity than other missions in sight.

In the light of our sensitivity we will need to do research for our phase metre that needs a resolution of $10^{-9}\,\text{rad}/\sqrt{Hz}$. Furthermore we will need to develop the corresponding laser to be used in our mission, check the thermal stability of materials and the mechanism to discharge the test mass.

After the technology development we will need to verify the instruments and their performance in our desired environment.

We are envisioning the start of the mission to take place not before 2026 and take an estimated 14-18 years. The time line is shown in figure 11.

9. Conclusions

The measurements by GLINT will provide extensive data on black holes, which will decrease the parameter space for the models of formation and evolution of these incredibly massive objects. The range in spacetime studied in this mission is a part that has never been directly detected, and this mission will fill in these blanks. GLINT also has the ability to constrain the cosmological models and

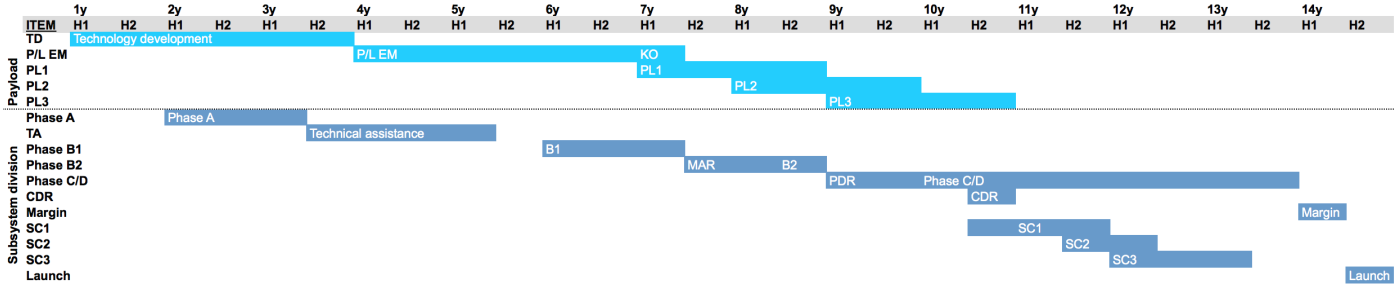

Figure 11: Timeline.

increase our understanding of one of the most fundamental laws of physics - gravitation.

Gravitational waves is a new revolutionary method for studying our Universe. Utilizing gravitational waves for studying the Universe rapidly widens the measurement range and will have an extensive impact on the research within fundamental physics and astrophysics, as well as corroborate our current view of the Universe, as obtained by electromagnetic radiation.

The engineering aspects of the GLINT project are very challenging because they require very well evolved technologies to limit the noise in the instruments. Even if those technologies need to be improved in order to give an answer to the requirements made, this work paves the way for a promising future in gravitational waves detection by identifying the potential sources of errors in the measurement process and quantifying them thoroughly. Different options for the detection have been studied during the engineering process such as the use of Bose-Einstein condensates, atomic clocks or Fabry-Pérot cavity to detect gravitational waves. Various trade-off have been made in order to identify key technologies to cope with the high accuracy required and to judge the technological readiness level of the instruments studied. This project has also developed concepts for constellation flight of satellites and a new structural design for spacecrafts.

The GLINT mission possesses the ability to expand the current technologies associated with laser interferometry and spacecraft design. Besides this GLINT will also provide the human race with new unknown information about the history of the Universe.

Acknowledgements

We would like to thank the European Space Agency, FFG and ISSI for their support. We would also like to thank all the summer school tutors, especially Christian Killow, Vitali Müller, Oliver Jennrich and Jose Sanjuán. And, of course, Martin Gehler, for his support and help. Without them, we would not have been able to attain the level that our space mission have reached today.

References

Airbus. 2003, Space Propulsion for the Access, Utilisation and Exploration of Space

Amaro-Seoane, P., Aoudia, S., Babak, S., et al. 2012, Classical and Quantum Gravity, 29, 124016

Armstrong, J., Estabrook, F., & Tinto, M. 2002, Time-Delay Interferometry

Barke, S. 2015

Bender, P. 1998, LISA : Laser Interferometer Space Antenna for the Detection and Observation of Gravitational Waves : Pre-phase A Report (Max-Planck-Institut fur Quantenoptik)

Danzmann, K. e. a. 2011

DeBra, D. B. 1997, Classical and Quantum Gravity, 14, 1549

Fryer, C. L., Holz, D. E., & Hughes, S. A. 2002, ApJ, 565, 430

Funakki, I. & Nakayama, Y. 2011, in Presented at the 32nd International Electric Propulsion Conference, Vol. 308, IEPC

Graham, P. W., Hogan, J. M., Kasevich, M. A., & Rajendran, S. 2013, Phys. Rev. Lett., 110, 171102

Hulse, R. A. & Taylor, H. J. 1974, in Bulletin of the American Astronomical Society, Vol. 6, Bulletin of the American Astronomical Society, 453

Livas, J., Thorpe, J., Numata, K., et al. 2009, Classical and Quantum Gravity, 26, 094016

Madau, P., Haardt, F., & Dotti, M. 2014, ApJS, 784, L38

Marcuccio, S. & Genovese, A. 1998, Journal of Propulsion and Power, 14, 774

Mohapatra, S., Cadonati, L., Caudill, S., et al. 2014, PhRvD, 90, 022001

Neal, P. 2015, Annenberg Learner, Teacher resources and professional developement across the curriculum

Ott, C. D., Burrows, A., Dessart, L., & Livne, E. 2006, Physical Review Letters, 96, 201102

Pacucci, F., Ferrara, A., & Marassi, S. 2015, MNRAS, 449, 1076

Perez, E. 2011, Ariane 5 User's Manual Issue 5 Revision 1

Petrich, L. I., Shapiro, S. L., & Wasserman, I. 1985, ApJS, 58, 297

Planck Collaboration, Ade, P. A. R., Aghanim, N., et al. 2014, , 571, A16

Ricotti, M. & Park, K. 2012, in American Institute of Physics Conference Series, Vol. 1480, American Institute of Physics Conference Series, ed. M. Umemura & K. Omukai, 297–302

Sabin, C., Bruschi, D. E., Ahmadi, M., & Fuentes, I. 2014, New Journal of Physics, 16, 085003

Saijo, M. 2011, PhRvD, 83, 124031

Schilling, J. 2009, Silverbird Astronautics

Schneider, R., Ferrara, A., Ciardi, B., Ferrari, V., & Matarrese, S. 2000, MNRAS, 317, 385

Shaddock, D. A., Ware, B., Spero, R., & Vallisneri, M. 2008, Post-processed time-delay interferometry for LISA

Wu, X.-B., Wang, F., Fan, X., et al. 2015, Nature, 518, 512

Yagi, K. 2013, International Journal of Modern Physics D, 22, 41013

Yue, B., Ferrara, A., Salvaterra, R., Xu, Y., & Chen, X. 2014, MNRAS, 440, 1263